# Effects of Contact Ratios on Mesh Stiffness of Helical Gears for Lower Noise Design

Lan Liu, Yunfei Ding, Liyan Wu and Geng Liu

In this paper, the influences of various gear parameters on the mesh stiffness are systematically investigated by using the finite element method. The comprehensive analysis shows that contact ratios are the key factors affecting the fluctuation value of mesh stiffness.

## Introduction

Gear transmission has been widely used in mechanical equipment as one of the most important transmission modes. The vibration and noise of gearsets is directly related to the whole characteristics of the transmission system. In order to improve the performance and reduce the noise of gear transmission system, more attention should be paid to the gear dynamics. The fluctuation of mesh stiffness is one of the most important internal excitations of gear transmission, so it is crucial issue to find the influence factors of mesh stiffness fluctuation (Ref. 1). Many scholars have performed a lot of work to investigate the mesh stiffness for general gears using theoretical and experimental methods (Refs. 2-5). The main result told that when the contact ratio is an integer that the stiffness is approximately constant, which has a low effect on the dynamic characteristics (Ref. 4). Liu (Ref. 6) and Bu (Ref. 7) discussed the influence of design parameters such as helix angle, pressure angle, tooth face width, etc. on the mesh stiffness. Related research focused on the relationship between mesh stiffness and gears basic parameters, which were not involved how to adjust the parameters to reduce the mesh stiffness fluctuations and achieve a lower noise level.

In this paper, the mesh stiffness and its fluctuation value of helical gears with different parameters are calculated respectively by using the finite element method. The gear parameters concerned include pressure angle, helical angle, addendum coefficient and face width and etc.. Since the mesh stiffness fluctuation is closely related to the loads variation on the contact lines, the model for solving the mean length, total length and time-varying length of contact lines is also established. Then the influences of various gear parameters on the mesh stiffness are systematically investigated. The comprehensive analysis of the mesh stiffness shows that contact ratios are the key factors affecting the fluctuation value of mesh stiffness when the gear parameters are changed. By optimizing the basic parameters of helical gears, the fluctuation of the mesh stiffness of helical gears can be reduced.

## Method for Calculating Mesh Stiffness

A modified method for determining the time-varying mesh stiffness and actual load distribution based on linear programming is used in this research referring to the literature (Ref. 8). Using *Pro/E*. software, a 3-D model of gear with true involutes profile was established based on the gear manufacturing technology firstly. Then the flexibility coefficient matrix of gear tooth surface was obtained using the substructure method by *ANSYS* software. Finally the time-varying meshing stiffness was solved by using linear programming method. The 3-D geometry and finite element models are presented in Figure 1. The advantage of this method is that the whole process is parameterized. In this method, the load

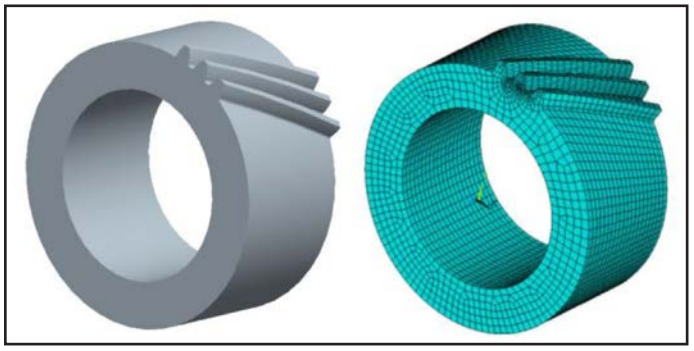

**Figure 1 3-D and finite element models of helical gear.**

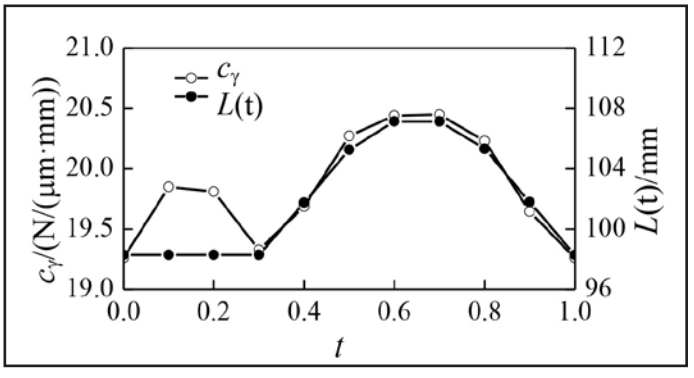


**Figure 2 Time-varying mesh stiffness in a mesh period.**

This paper was originally presented at the 2014 International Gear Conference, Lyon Villeurbanne, France and is republished here with the authors' permission.

distribution along the contact lines and mesh stiffness during the whole meshing period can be evaluated simultaneously.

Figure 2 shows the time-varying mesh stiffness in a mesh period calculating by the finite element method mentioned above. The $x$ coordinate $t$ means dimensionless time which is the mesh time divided by one mesh period. The $y$ coordinate $c_\gamma$ and $L(t)$ are the time-varying mesh stiffness and the time-varying contact-line length respectively. The meshing stiffness decreases at the instantaneous position where the teeth enter contact or exit contact.

In order to study the laws of mesh stiffness, its fluctuation $\eta_{c\gamma}$ is defined as follows:

$$\eta_{c\gamma}=\frac{\Delta c_\gamma}{c_{\gamma m}}\times 100\% \tag{1}$$

where $c_{\gamma m}$ is the mean value of the time-varying mesh stiffness in one whole mesh period. The symbol $\Delta c_\gamma$ is the difference value between the maximum value $c_{\gamma max}$ and minimum value $c_{\gamma min}$ of the time-varying mesh stiffness, i.e. — $\Delta c_\gamma = c_{\gamma max} - c_{\gamma min}$.

## Fluctuation of Contact-Line Length

Figure 3 shows the action plane of a pair of helical gears and the contact lines at different meshing times. Gear teeth begin to meshing from $A$ position and out of meshing at $C$ position. The line $AD$ represents the actual action line, and line $CD$ means the tooth face width $B$, where $\varepsilon_\alpha$ and $\varepsilon_\beta$, being the transverse contact ratio and overlap contact ratio, respectively, and $p_{bt}$ and $p_{ba}$ being the transverse base pitch and axle base pitch, respectively. $\beta_b$ is the base helix angle.

The formulas of contact-line length are derived based on Figure 3, which include the time-varying total contact-line length within the action plane $L(t)$, the mean value of the total contact-line length $L_m$, the maximum value $L_{max}$, and minimum value $L_{min}$. Here we define $E_\alpha$ and $E_\beta$ as representing the integer part of $\varepsilon_\alpha$ and $\varepsilon_\beta$, while we define $e_\alpha$ and $e_\beta$ as representing the decimal part of $\varepsilon_\alpha$ and $\varepsilon_\beta$ respectively.

If $e_\alpha + e_\beta \le 1$, the time-varying length $L(t)$ can be expressed as:

$$L(t)=L_1+\begin{cases}\dfrac{p_{ba}}{\cos\beta_b}t & 0\le t<e_1\\ \dfrac{p_{ba}e_1}{\cos\beta_b}t & e_1\le t\le e_2\\ \dfrac{p_{ba}}{\cos\beta_b}(-t+e_1+e_2) & e_2<t\le e_1+e_2\\ 0 & e_1+e_2<t\le 1\end{cases} \tag{2}$$

While, $e_\alpha + e_\beta > 1$:

$$L(t)=L_1+\begin{cases}\dfrac{p_{ba}}{\cos\beta_b}(e_1+e_2-1) & 0\le t<e_1+e_2-1\\ \dfrac{p_{ba}}{\cos\beta_b}t & e_1+e_2-1\,t\le e_1\\ \dfrac{p_{ba}e_1}{\cos\beta_b} & e_1<t\le e_2\\ \dfrac{p_{ba}}{\cos\beta_b}(-t+e_1+e_2) & e_2<t\le 1\end{cases} \tag{3}$$

Where: $L_1 = E_\alpha E_\beta l_1(t) + E_\beta l_2(t) + E_\alpha l_3(t)$, $l_1(t) = p_{ba}/\cos\beta_b$, $l_2(t) = p_{ba}e_\alpha/\cos/\beta_b$, $l_3(t) = p_{ba}e_\beta/\cos\beta_b$, $e_1 = minv(e_\alpha, e_\beta)$ and $e_2 = \max(e_\alpha, e_\beta)$.

The mean value $L_m$ of the contact-line length can be given by:

$$L_m=\frac{\varepsilon_\alpha B}{\cos\beta_b}=\frac{\varepsilon_\alpha\varepsilon_\beta p_{ba}}{\cos\beta_b} \tag{4}$$

According to Equations 2 and 3, the maximum value $L_{max}$ of the contact-line length can be derived as:

$$L_{min}=\frac{(\varepsilon_\alpha\varepsilon_\beta - e_\alpha e_\beta + e_1)\,p_{ba}}{\cos\beta_b} \tag{5}$$

When $e_\alpha + e_\beta \le 1$, the minimum value $L_{min}$ of the contact-line length can be expressed as:

$$L_{min}=\frac{(\varepsilon_\alpha\varepsilon_\beta - e_\alpha e_\beta)\,p_{ba}}{\cos\beta_b} \tag{6}$$

while $e_\alpha + e_\beta > 1$, the minimum value $L_{min}$ of the contact-line length can be expressed as:

$$L_{min}=\frac{(\varepsilon_\alpha\varepsilon_\beta - e_\alpha e_\beta + e_\alpha + e_\beta - 1)\,p_{ba}}{\cos\beta_b} \tag{7}$$

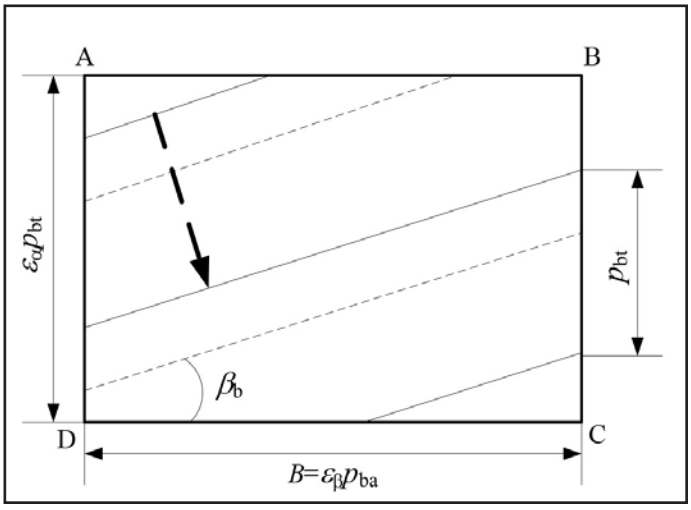


**Figure 3 Action plane and contact lines.**

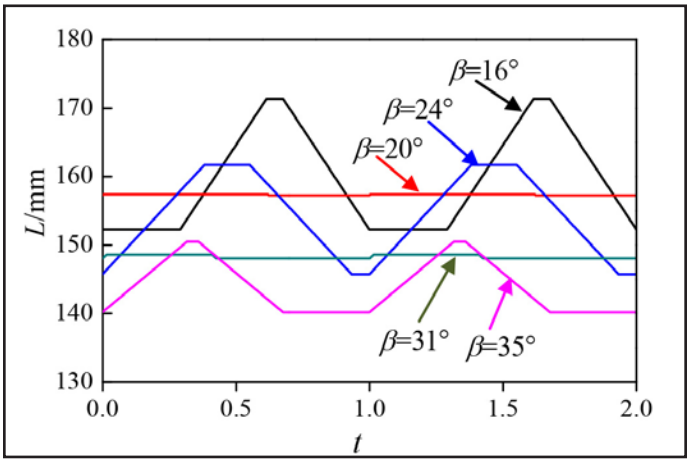


**Figure 4 Lengths of contact lines vs. different helix angles β.**

In order to measure the fluctuation of contact-line length during one whole meshing period, the changing ratio of the total length of contact lines $\eta_L$, defined as the relative difference between the maximum value $L_{max}$ and the minimum value $L_{min}$ to the mean value $L_m$ of the total length of contact lines. The formula of $\eta_L$ is expressed as:

$$\eta_L = \frac{L_{max} - L_{min}}{L_m} \times 100\% \quad (8)$$

On the basis of Equations 4–7, $\eta_L$ can also be expressed as:

$$\eta_L = \begin{cases} \frac{e_1}{\varepsilon_\alpha \varepsilon_\beta} \times 100\% & \varepsilon_\alpha + \varepsilon_\beta \le 1 \\ \frac{1 - e_2}{\varepsilon_\alpha \varepsilon_\beta} \times 100\% & \varepsilon_\alpha + \varepsilon_\beta > 1 \end{cases} \quad (9)$$

Figure 4 shows the effects of helix angle β on the time-varying contact lines. Table 1 displays the initial parameters of the helical gears that are discussed in Figure 5. The helix angle β is varied from 16° – 35°. It is seen that the variation of curves has the same trend — but with different amplitudes. Comparing contact ratios at different helix angles, as seen in Table 2, it is found that when the overlap contact ratio of a helical gear is close to an integer, such as when β is 20° or is 31°, the amplitude of $L(t)$ is very low, and the changing ratio of the total length of contact lines $\eta_L$ is approximate to zero.

**Table 1 The parameters of helical gears**

| parameter | $z$ | $m_n$/mm | $\alpha_n$/° | $\beta$/° | $h_{an}$ | $c_n$ | $B$/mm | $x$ |
|---|---|---|---|---|---|---|---|---|
| pinion | 37 | 5 | 20 | 16~35 | 1.0 | 0.25 | 92 | 0 |
| gear | 106 | 5 | 20 | 16~35 | 1.0 | 0.25 | 92 | 0 |

**Table 2 Contact ratios at different helix angles**

| $\beta$/° | $\varepsilon_\alpha$ | $\varepsilon_\beta$ | $\varepsilon_\gamma$ |
|---|---|---|---|
| 16 | 1.6760 | 1.6411 | 3.2904 |
| 20 | 1.6197 | 2.0032 | 3.6229 |
| 24 | 1.5523 | 2.3822 | 3.9346 |
| 31 | 1.4104 | 3.0165 | 4.4269 |
| 35 | 1.3175 | 3.3594 | 4.6769 |

In order to reveal the rules of the length of contact lines, considering the general conditions, the surface chart about the changing ratio of the total length of contact lines $\eta_L$ vs. different transverse contact ratios and overlap contact ratios is plotted in Figure 5; this curved surface chart is obtained by the Equation 9.

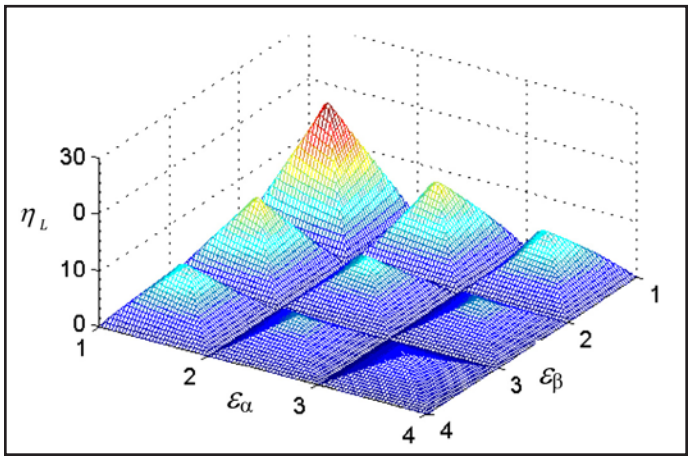


**Figure 5 The surface chart of $\eta_L$ vs. contact ratios.**

From Figure 5 the influences of contact ratios, including transverse contact ratio, overlap contact ratio and total contact ratio to the length of contact line are exhibited. The results show that contact ratios are the key factor affecting the fluctuation value of contact-line length. The fluctuation value of $\eta_L$ has an extreme maximum when the total contact ratio is an integer, while it has a minimum, i.e. — zero — when the transverse contact ratio or face contact ratio is an integer.

## The Influential Factors of Mesh Stiffness

In order to discuss the influential factors of mesh stiffness and its fluctuation, a series of mean values of the time-varying mesh stiffness $c_{\gamma m}$ and their fluctuation values $\eta_{c\gamma}$, mean values of contact-line length $L_m$ and their changing ratios $\eta_L$ of helical gears with different parameters were solved, respectively, using the method mentioned above.

***Helix angle.*** Figure 6 shows the effect of helix angle β on the mean value of mesh stiffness $c_{\gamma m}$ and contact-line length $L_m$. The helix angle β is varied from 14° – 42°. It is seen that the mean values of mesh stiffness and lengths of contact lines decrease in the same trend while helix angle β increases.

Figure 7 shows that the changing ratio of the total length of contact lines $\eta_L$ and mesh stiffness $\eta_{c\gamma}$ change with the contact ratios when helix angle β increases. The overlap contact ratio is varied from 1.41 – 3.91, while the total contact ratio varying from 3.11 – 5.06 when β increased from 14° – 42°. It is seen that mesh stiffness and lengths of contact lines have the same trend, while helix angle β or contact ratios increase.

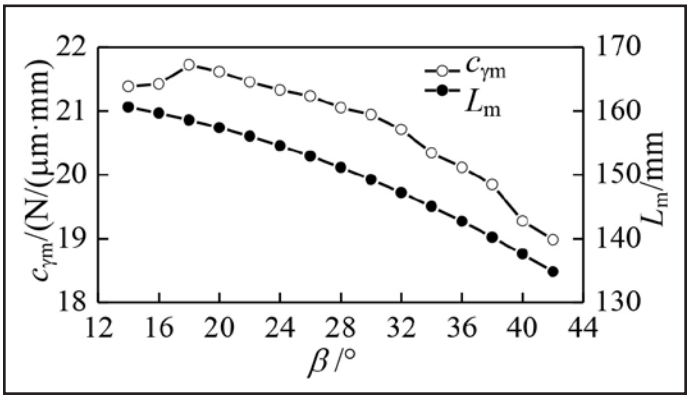


**Figure 6 The $c_{\gamma m}$ and $L_m$ vs. different helix angles β.**

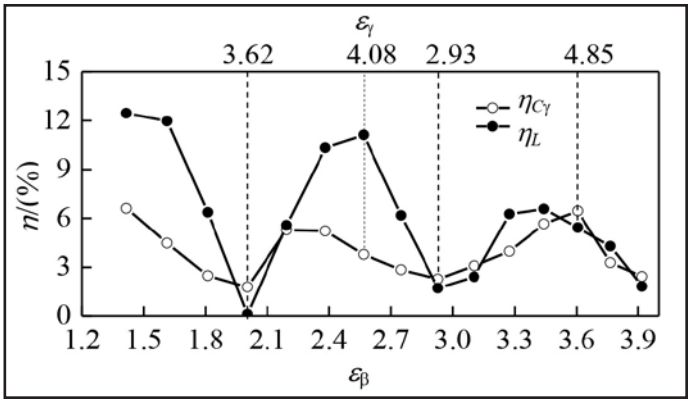


**Figure 7 The $\eta_{c\gamma}$ and $\eta_L$ vs. helix angle and contact ratios.**

The graph shows that the minimum value of $\eta_{c\gamma}$, as well as $\eta_L$, appears when the overlap contact ratio is close to an integer. However the maximum value of $\eta_{c\gamma}$ and $\eta_L$ appears when the total contact ratio is close to an integer.

***Addendum coefficient.*** Figure 8 shows the effect of addendum coefficient $h_{an}$ on the mean value of mesh stiffness $c_{\gamma m}$ and contact-line length $L_m$; the addendum coefficient $h_{an}$ is varied from 0.4 – 1.4. It is seen that the mean values of mesh stiffness and lengths of contact lines increase in the same trend when addendum coefficient $h_{an}$ increases. The increasing values of $L_m$ and $c_{\gamma m}$ are 144 mm and 8.37 N/(μm·mm), respectively.

Figure 9 shows the changing ratio of the total length of contact lines $\eta_L$ and mesh stiffness $\eta_{c\gamma}$ change with the contact ratios when addendum coefficient $h_{an}$ increases. The transverse contact ratio is varied from 0.63 – 2.05, while the overlap contact ratio remains unchanged, and the total contact ratio varying from 3.26 – 4.68 when $h_{an}$ increases from 0.4 – 1.4. The graph shows that the minimum value of $\eta_{c\gamma}$, as well as $\eta_L$, appear when the transverse contact ratio is close to integer, which is 1 or 2 here. However, the maximum value of $\eta_{c\gamma}$ and $\eta_L$ appears when the total contact ratio is close to integer 4.

***Tooth face width.*** Figure 10 shows the effect of tooth face width on the mean value of mesh stiffness $c_{\gamma m}$ and contact-line length $L_m$. The face width $B$ is varied from 52 mm – 118 mm. It is seen that $c_{\gamma m}$ and $L_m$ increase in the same trend when the face width $B$ increases. The increasing values of $L_m$ and $c_{\gamma m}$ are 109 mm and 3.19 N / ($\mu m \cdot mm$), respectively.

The results of $\eta_{c\gamma}$ and $\eta_L$, by varying the tooth face width $B$ from 52mm to 118mm, are plotted in Figure 11, which shows that $\eta_L$ and $\eta_{c\gamma}$ change with the contact ratios when face width $B$ increases. The overlap contact ratio is varied from 1.48 – 3.37 while the transverse contact ratio remains the same, and the total contact ratio varying from 2.99 – 4.87.

The graph shows that the minimum value of $\eta_{c\gamma}$ — as well as $\eta_L$ — appears when the overlap contact ratio is close to an integer — 2 or 3 in this case. But the maximum value of $\eta_{c\gamma}$ and $\eta_L$ appears when the total contact ratio is close to integer 4.

***Pressure angle.*** Figure 12 shows the effect of gear pressure angle $\alpha_n$ on the mean value of mesh stiffness $c_{\gamma m}$ and contact-line length $L_m$. The pressure angle $\alpha_n$ is varied from 16° – 26°. It is seen that the mean values of mesh stiffness and lengths of contact lines decrease in the same trend when pressure angle $\alpha_n$ increases. The decreasing values of $L_m$ and $c_{\gamma m}$ are 46.98mm and 1.41N/ (μm·mm), respectively.

The results of $\eta_{c\gamma}$ and $\eta_L$ by varying the pressure angle $\alpha_n$ from16° to 26° are plotted in Figure 13, which shows that $\eta_L$ and $\eta_{c\gamma}$ change with the contact ratios when pressure angle $\alpha_n$ increases. The transverse contact ratio is varied from 1.73 – 1.29, while the overlap contact ratio is unchanged, and the total contact ratio varying from 4.36 – 3.92.

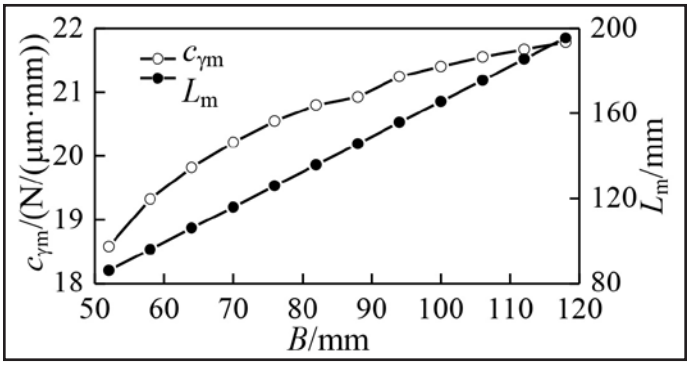


**Figure 10 The $c_{\gamma m}$ and $L_m$ vs. different face width $B$.**

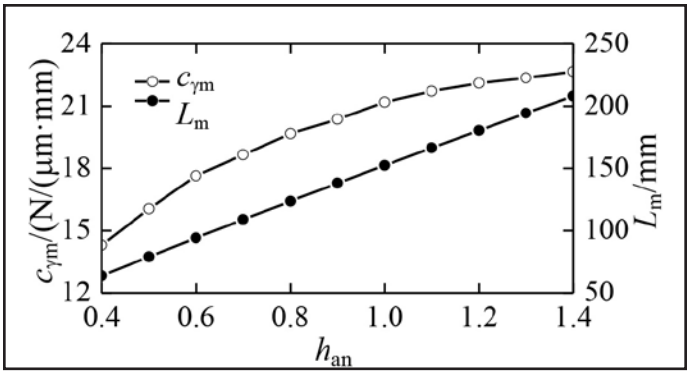


**Figure 8 The $c_{\gamma m}$ and $L_m$ vs. different addendum coefficient $h_{an}$.**

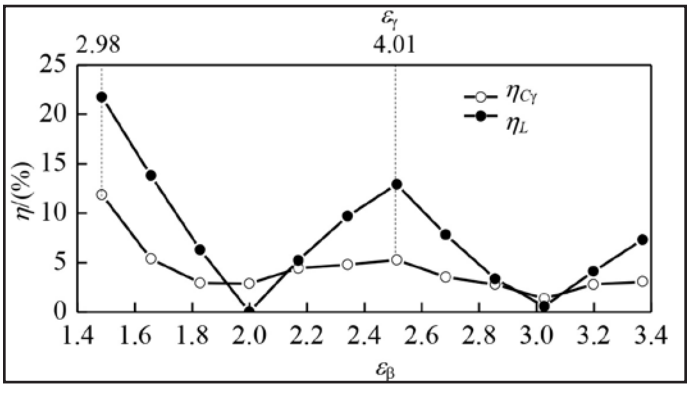


**Figure 11 The $\eta_{c\gamma}$ and $\eta_L$ vs. face width and contact ratios.**

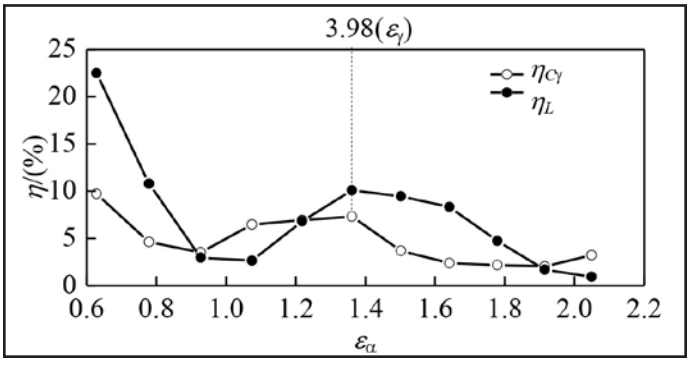


**Figure 9 The $\eta_{c\gamma}$ and $\eta_L$ vs. addendum coefficient and contact ratios.**

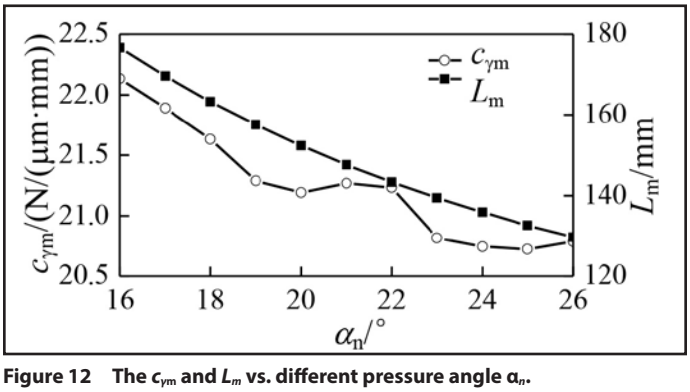


**Figure 12 The $c_{\gamma m}$ and $L_m$ vs. different pressure angle $\alpha_n$.**

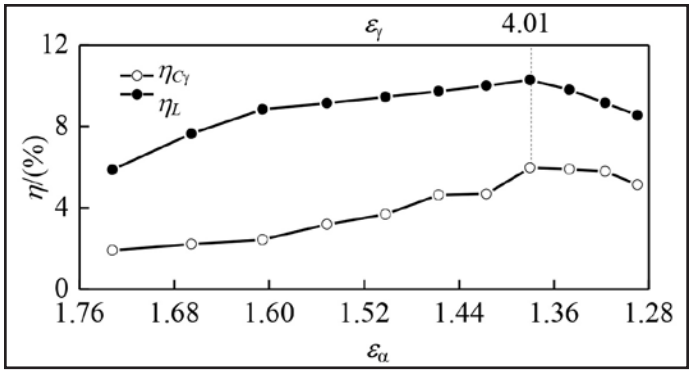


**Figure 13 The $\eta_{c\gamma}$ and $\eta_L$ vs. pressure angle and contact ratios.**

Here the graph doesn't show that the minimum value of $\eta_{c\gamma}$ or $\eta_L$ appears when the overlap contact ratio is an integer because of the pressure angle range. However, the maximum value of $\eta_{c\gamma}$ and $\eta_L$ appears when the total contact ratio is close to integer 4. Regardless of calculating errors, the trend of $\eta_{c\gamma}$ is completely the same as $\eta_L$.

## Conclusions

In this paper the mesh stiffness and its fluctuation value of helical gears with different parameters, respectively, are calculated by using the finite element method. The influences of various gear parameters on the mesh stiffness are systematically investigated. The gear parameters concerned here include pressure angle, helical angle, addendum, co-efficient, face width, etc. The comprehensive analysis of the mesh stiffness shows that contact ratios are the key factors affecting the fluctuation value of mesh stiffness when the gear parameters are changed. The fluctuation value of mesh stiffness attains a minimum when the transverse contact ratio or overlap ratio is close to an integer, while it has an extreme maximum when the total contact ratio is approximate to an integer.

Since mesh stiffness fluctuation is closely related to the load variations on the contact lines, the model for solving the mean length, total length and time-varying length of contact lines is also established. By calculating the length of contact lines of various helical gear pairs with different basic parameters, the results show that the total length of contact lines doesn't change when the transverse contact ratio or overlap ratio is an integer, while it fluctuates more intensively when the total contact ratio is indeed an integer.

In comparing the fluctuation amplitude of the total length of contact lines with the fluctuation amplitude of mesh stiffness, it is found that the fluctuation amplitudes of both contact lines and mesh stiffness have the same trend when gear parameters are changed. So it is proposed that the length and fluctuation value of contact line can be used to approximately measure the trend of mesh stiffness — but the values of mesh stiffness still need special calculation software.

According to the above discussion, it can be predicted that by optimizing the basic parameters of helical gears, the fluctuation of the mesh stiffness of helical gears can be reduced and the gear transmission system with appropriate contact ratios can achieve a lower vibration and noise level. **PTE**

**Acknowledgment.** *This work is supported by the 111 project (Grant No.B13044) and the Engineering Research Center of Expressway Construction & Maintenance Equipment and Technology (Chang'an University), MOE (2013G1502057).*

## References

1. Smith, J.D. *Gear Noise and Vibration*, Marcel Dekker, Inc., New York, 2003.
2. Umezawa, K., T. Suzuki and T. Sato. *Bulletin of JSME.* 29, 1605-1611, 1986.
3. Nagaya, K. and S. Uematsu. *Trans. ASME. J. Mech. Des.* 103, 357-363, 1981.
4. Maclennan, L.D. *J. Mechanical Engineering Science,* 216, 1005-1016, 2002.
5. Wang, J and I. Howard. *J. Mechanical Engineering Science,* 218, 131-142, 2004.
6. Liu, G. *Chinese Journal of Mechanical Engineering,* 27, 20-24, 1991.
7. Bu, Z.H., G. Liu and L. Y. Wu. *Journal of Aerospace Power (Chinese),* 25, 957-962, 2010.
8. Bu, Z.H., G. Liu., L. Y. Wu and Z. M. Liu. *Mechanical Science and Technology for aerospace Engineering (Chinese),* 27, 1365-1368, 2008.

**Lan Liu** received his PhD in mechanical engineering in 2007 at the Northwestern Polytechnical University of China, and then joined the University the following year as an associate professor of mechanical engineering. His current research interests include the dynamics and vibro-acoustics of gear system, advanced numerical simulation methods and bionic mechanics. Liu is now teaching theory of elasticity and finite element method.

**Yunfei Ding** was a postgraduate student in mechanical engineering when he as co-author for this paper. He has received his master degree in 2014 at the Northwestern Polytechnical University of China.

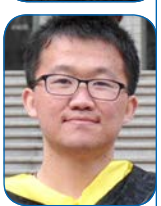

**Liyan Wu** is professor of mechanical engineering at the Northwestern Polytechnical University of China. His current research interests include the reliability techniques in machine design, control technology for vibration and noise in mechanical system and modern theories and methods in machine design.

**Geng Liu** is professor of mechanical engineering at Northwestern Polytechnical University of China. He holds a PhD in mechanical engineering since 1994 from Xian Jiaotong University of China. From 1997-1999, he has as visiting scholar and post-doctoral fellow studied in Florida International University and Northwestern University of USA respectively. His current research interests include contact mechanics, mechanical transmission and virtual and physical prototyping simulation of mechanical systems.